

# Simulating Magnetic Monopoles

## by Extending GEANT

G. Bauer M.J. Mulhearn<sup>b</sup> Ch. Paus P. Schieferdecker  
S. Tether

*Massachusetts Institute of Technology,  
Department of Physics, Laboratory for Nuclear Science,  
Bldg. 26-505, 77 Massachusetts Avenue, Cambridge, MA 02139-4307, U.S.A.*

<sup>b</sup>*Proofs: Michael Mulhearn, FNAL PO Box 500 MS 318, Batavia, IL 60510  
(630) 840-8412, mulhearn@mit.edu.*

---

### Abstract

GEANT is a widely used tool for detector description and simulation, but does not handle particles with magnetic charge. In this article we describe an extension to track a simple monopole having magnetic charge, but no electric charge or hadronic interactions.

*Key words:* Magnetic Monopoles, Simulation, GEANT

*PACS:* 14.80.Hv, 07.05.Tp

---

---

*Email addresses:* [bauerg@fnal.gov](mailto:bauerg@fnal.gov) (G. Bauer), [mulhearn@mit.edu](mailto:mulhearn@mit.edu)

# 1 Introduction

The existence of magnetic monopoles would add symmetry to the Maxwell equations without breaking any known physical law. More dramatically, it would make charge quantization a consequence of angular momentum quantization, as first shown by Dirac [1]. With such appeal, monopoles continue to excite interest and new searches despite their elusiveness to date.

Grand unified theories predict monopole masses of about  $10^{17}$  TeV, so there have been extensive searches for high mass monopoles produced by cosmic rays [2a–c]. Indirect searches for low mass monopoles have looked for the effects of virtual monopole loops added to QED Feynman diagrams [3a–d]. Detector materials exposed to radiation from  $p\bar{p}$  collisions at the Tevatron have been examined for trapped monopoles [4]. All results have been negative [5].

In this article we consider the possible production and detection of Dirac monopoles with mass less than 1 TeV in a present day collider experiment. By a Dirac monopole, we mean a particle bearing no electric charge, having no hadronic interactions, and whose magnetic charge  $g$  satisfies the Dirac quantization condition<sup>1</sup>:

$$\frac{ge}{\hbar c} = \frac{n}{2} \iff \frac{g}{e} = \frac{n}{2\alpha} . \quad (1)$$

If produced inside a particle detector, a monopole would be revealed by its unique characteristics. Because a magnetic charge is accelerated along an ex-

(M.J. Mulhearn), [paus@fnal.gov](mailto:paus@fnal.gov) (Ch. Paus ), [schiefer@fnal.gov](mailto:schiefer@fnal.gov)

(P. Schieferdecker ), [tether@fnal.gov](mailto:tether@fnal.gov) (S. Tether ).

<sup>1</sup> From here on we use Gaussian units with the additional convention of setting  $c$  to unity.

ternal magnetic field, the trajectories of monopoles and ordinary charged particles differ dramatically. From the Dirac quantization condition, the smallest magnetic charge would have a magnitude about 68.5 times greater than that of an electron or proton. For monopoles passing through matter, this causes high ionization and rapid energy loss.

## 2 Theory

The new symmetry lent to the Maxwell equations by the existence of magnetic monopoles can be exploited to obtain monopole versions of the Lorentz force, Bethe-Bloch equation, and other relations governing electromagnetic interactions with matter. These are the only theoretical results needed for the GEANT treatment of monopoles.

For those of us searching for monopoles at particle accelerators, there remains the vexing question of production cross sections. Refs. [6a–c] describe scattering cross sections for the general case of particles with arbitrary EM charge, but explains that the monopole’s large coupling to the EM field renders perturbative techniques useless. Any attempt to puzzle out an answer based on Feynman diagrams and considerations of duality and Lorentz invariance is doomed to failure. There is presently no reliable field theoretical calculation of monopole production cross sections. As a benchmark for testing, we adopt a Drell-Yan like monopole pair production mechanism motivated by the new symmetry, as in Ref. [4].

## 2.1 The Duality Transformation

The Maxwell equations extended to include magnetic charge take the following form:

$$\begin{aligned}
 \vec{\nabla} \cdot \vec{D} &= 4\pi\rho_e & (2) \\
 \vec{\nabla} \cdot \vec{B} &= 4\pi\rho_m \\
 -\vec{\nabla} \times \vec{E} &= \frac{\partial}{\partial t}\vec{B} + 4\pi\vec{j}_m \\
 \vec{\nabla} \times \vec{H} &= \frac{\partial}{\partial t}\vec{D} + 4\pi\vec{j}_e,
 \end{aligned}$$

where  $\rho_m$  is the magnetic charge density and  $\vec{j}_m$  is the corresponding current. The form of these equations is invariant under a general duality transformation ( $\xi \in \mathfrak{R}$ ):

$$\begin{aligned}
 \vec{E} &= \vec{E}' \cos \xi + \vec{H}' \sin \xi & \vec{D} &= \vec{D}' \cos \xi + \vec{B}' \sin \xi & (3) \\
 \vec{H} &= -\vec{E}' \sin \xi + \vec{H}' \cos \xi & \vec{B} &= -\vec{D}' \sin \xi + \vec{B}' \cos \xi \\
 \rho_e &= \rho'_e \cos \xi + \rho'_m \sin \xi & \vec{j}_e &= \vec{j}'_e \cos \xi + \vec{j}'_m \sin \xi \\
 \rho_m &= -\rho'_e \sin \xi + \rho'_m \cos \xi & \vec{j}_m &= -\vec{j}'_e \sin \xi + \vec{j}'_m \cos \xi.
 \end{aligned}$$

The original Maxwell equations are recovered if all particles have the same ratio of magnetic charge to electric charge, which can be set to zero by the right choice of the angle  $\xi$ . A useful special case of the duality transformation is when  $\xi = \pi/2$ ; the extended Maxwell equations are invariant under the replacements

$$\begin{aligned}
 \rho_e &\rightarrow \rho_m & \vec{j}_e &\rightarrow \vec{j}_m & \vec{E} &\rightarrow \vec{H} & \vec{D} &\rightarrow \vec{B} & (4) \\
 \rho_m &\rightarrow -\rho_e & \vec{j}_m &\rightarrow -\vec{j}_e & \vec{B} &\rightarrow -\vec{D} & \vec{H} &\rightarrow -\vec{E},
 \end{aligned}$$

which can be used to derive monopole versions of formulas familiar from standard classical electrodynamics. This is the transformation meant by “duality” or the “dual” of an EM quantity.

## 2.2 Motion in a Magnetic Field

Duality implies a generalized Lorentz force law for particles carrying arbitrary electric charge  $e$  and magnetic charge  $g$ :

$$\vec{F} = e \left( \vec{E} + \vec{\beta} \times \vec{B} \right) + g \left( \vec{B} - \vec{\beta} \times \vec{E} \right) . \quad (5)$$

Setting  $e$  and  $\vec{E}$  to zero provides the differential equation describing the motion of a Dirac monopole in a magnetic field. It can be solved analytically for the case of a uniform field, but the general case requires a numerical integration. We have implemented both solutions in GEANT for efficiency and to provide an additional cross check (see Section 4.2).

The most distinctive features of the monopole kinematics are that the trajectory does not curve in the plane perpendicular to the magnetic field, and the field does work on the monopole.

## 2.3 Ionization and Delta Rays

The energy loss,  $dE/dx$ , due to ionization for an electrically charged particle is given by the Bethe-Bloch formula [7],

$$-\frac{dE}{dx} = z^2 \frac{KZ}{A} \frac{1}{\beta^2} \left[ \frac{1}{2} \ln \left( \frac{2m_e \beta^2 \gamma^2}{I^2} \right) - \beta^2 \right] , \quad (6)$$

where  $K/A = 4\pi N_A r_e^2 m_e c^2 / A = 0.000307 \text{ GeV cm}^2/\text{g}$  and  $I$  is the mean excitation energy of the scattering material, roughly  $Z \cdot 10 \text{ eV}$ .

This formula is derived by considering the impulse imparted to an electron in the material by the passage of the charged particle [8]. Replacing the EM field tensor for a moving electric charge by its dual shows that the only field component that delivers a net impulse to the electron is an electric field proportional to both the monopole charge  $ng$  and its speed  $\beta$ . The net effect is to replace  $ze$  by  $ng\beta$ :

$$-\frac{dE}{dx} = (ng/e)^2 \frac{KZ}{A} \left[ \frac{1}{2} \ln \left( \frac{2m_e \beta^2 \gamma^2}{I^2} \right) - \beta^2 \right]. \quad (7)$$

The same conclusion is reached by considering the generalized non-relativistic scattering cross section for small scattering angles [9a-c]. The familiar result for electric-electric scattering (Rutherford scattering),

$$\frac{d\sigma}{d\Omega} \approx \frac{1}{2m\beta} \frac{(ze)^2}{\beta^2} \frac{1}{(\theta/2)^4}, \quad (8)$$

becomes for magnetic-electric scattering

$$\frac{d\sigma}{d\Omega} \approx \frac{1}{2m\beta} (ng)^2 \frac{1}{(\theta/2)^4}, \quad (9)$$

where  $m$  is the mass of the light particle.

The ionization energy loss for a magnetic monopole in air is compared to an ordinary charged particle in Figure 3. There are two differences: the monopole curve is flatter due to canceling of the  $1/\beta^2$  factor and higher due to the large value of  $g/e \approx 68.5$ . The large ionization energy loss means that the range of monopoles in most solid materials is quite short.

To an electron in matter, a passing monopole is effectively a passing nuclei of

charge  $z \sim n \cdot 68.5 \cdot \beta$ . The mean energy loss, energy loss fluctuations, and delta ray production are all different aspects of this interaction. The equations describing these phenomena are valid for a wide range of nuclei, up to  $z \sim 200$ . So for small values of  $n$ , the replacement  $ze \rightarrow ng\beta$  is justified.

#### *2.4 Multiple Scattering*

The formula for multiple scattering of monopoles from the nuclei of atoms is similarly deduced. By exactly the same exercise as before—replacing the EM tensor for an electron with its dual—the monopole multiple scattering formula is seen to have a factor  $ng\beta$  in place of  $ze$ . One can use any of the models for multiple scattering by making this replacement.

#### *2.5 Čerenkov Radiation*

Starting with the far fields of a moving charge (see Ref. [8]) and applying the duality transformation, one obtains the far fields for a moving monopole. The Poynting vector,  $(\vec{E} \times \vec{B})/4\pi$ , in the two cases differs only by a substitution of electric with magnetic charge. There is no  $\beta$  factor because both the electric and magnetic fields are involved, not just the electric field as in the interactions considered above. For Čerenkov radiation, one merely replaces electric charge with magnetic charge ( $ze \rightarrow ng$ ).

### 3 Modifications to GEANT

GEANT simulates particles passing through a detector, calculating each trajectory step by step, handling the motion in an arbitrary magnetic field, interactions with material in the detector, and decays of unstable particles.

Each step size is chosen small enough to accurately treat all processes independently. For instance, the energy loss continuously effects the trajectory, but for a small enough step size it can be calculated after the particle has been transported. GEANT uses path length, not time, as the independent variable in its integrations, a simplification mainly because material interactions have characteristic lengths.

The step size is taken from many constraints. For example, a large field gradient, strong trajectory curvature, or rapid energy loss reduces the size. When a step size cannot be estimated ahead of time, it is done iteratively; if a calculated effect is too large, the step is recalculated with a reduced size.

Discreet processes are handled differently. For an unstable particle, the proper lifetime is chosen at the start by drawing an exponentially distributed random number using the particle's mean lifetime as the parameter. At each step, the remaining proper lifetime and the particle's momentum are used to calculate a decay distance. If the step size eventually chosen is smaller than this distance, the elapsed proper time of the step is subtracted from the particle's remaining lifetime. Otherwise the step size is shortened to the decay distance and the decay process is performed at the end of the step.

Material interactions are handled in a similar fashion, with a random distance

drawn using the interaction length as a parameter. Because this is meaningful only if the interaction length of the material is constant, GEANT does not allow a step to cross a volume boundary. It handles this internally by treating boundary crossing as if it were another kind of interaction guaranteed to occur at the boundary.

### *3.1 Code Layout*

GEANT uses a modular design which allows different particles to share appropriate code. User entry points are provided using names beginning with **GU** (e.g. **GUTRACK**); the default behavior is to merely call GEANT code, but users can add their own special purpose code as needed.

Figure 1 shows a partial calling graph for GEANT tracking. Our additions, covered in detail below, are in the dashed box. There are three important divisions in this graph:

- (1) At the highest level, GEANT performs bookkeeping tasks and decides the appropriate code to call for each particle. Code for the entire event, **GUTREV** and **GTREVE**, calls generic code to step through one track, **GUTRAK** and **GTRACK**.
- (2) At the next level, the appropriate particle specific code—**GTGAMA**, **GTELEC**, **GTMUON**, **GTHADR**, **GTNEUT**, or **GTMONP**—is chosen by “tracking type” based on charge, mass, equations of motion, and the types of interactions considered. This code performs a single step, deciding the appropriate step size and handling interactions.
- (3) At the lowest level, the actual numerical integration of the equations of

motion is performed. A user routine—`GUSWIM` or `GUSWMP`— chooses which numerical integration—`GRKUTA`, `GHELIX`, `GHELX3`, `GPARMP`, or `GRKTMP`— to use based on the uniformity and strength of the magnetic field as calculated by the user supplied routine `GUFLD`.

Additional GEANT code, not shown in the calling graph, calculates physics processes such as energy loss fluctuations and multiple scattering. The particle specific tracking code selects appropriate physics processes to apply.

We add Dirac monopoles in a manner consistent with GEANT's organization. Because the equations of motion for magnetic monopoles and standard GEANT particles are completely different, we use a new tracking type, `ITRTYP= 9`, corresponding to routine `GTMONP` and alter `GTRACK` accordingly.

Normally in GEANT, the particle specific code calls `GUSWIM` to transport the particle. But the magnetic field does work on a magnetic charge, which is not true for electric charge, and the arguments given to `GUSWIM` do not allow the integration routines to alter the total energy. Rather than change `GUSWIM` and all code that calls it, we have `GTMONP` call a new similar routine `GUSWMP`. `GUSWMP` calls an appropriate numerical integration of the equations of motion: `GPARMP` for an analytic solution and `GRKTMP` for Runge-Kutta integration.

### *3.2 Monopole Tracking*

The main monopole tracking routine, `GTMONP`, is derived from the charged hadron tracking routine, `GTHADR`, but with decays, hadronic interactions, and stopping calculations omitted. The relevant kinematic parameters are the same for monopoles and hadrons, so no additional parameters are needed. New

energy loss and range tables are not needed; the already defined proton tables are adapted, as described in Section 3.3.

Figure 2 illustrates the monopole tracking algorithm. A step size is chosen based on the particle's position in the volume and material interactions. It is transported by the numerical integration, and the effects of interactions are calculated. If the effects are too large, the step size is reduced and the calculations are repeated.

In order to transport a monopole according to the kinematics of Section 2.2, a suitable numerical routine is chosen. For a constant magnetic field in the  $z$  direction, an analytic solution to the equations of motion, **GPARMP**, is used. A simple numerical integration is still needed to obtain the step size from the time based analytic solution. For non-uniform magnetic fields, a fourth order Runge-Kutta integration of the equations of motion, **GRKTMP**, is used. There are more efficient integration methods available but they are unreliable if the integrand is not guaranteed to be smooth [10]. That is usually the case for HEP applications, where the magnetic field map is often based on table lookups and split into several pieces, each covering a different region of the detector.

The step size is limited to ensure that the relative error in the total momentum at each step is less than one part in  $10^5$  (at the moment, this is hard coded). The safe step size estimate,  $\Delta s_{safe}$ , for a maximum relative error  $\delta$  is given by

$$\Delta s_{safe} = 7388 \cdot \frac{p^2}{gE|\vec{B}|} \delta^{1/5}. \quad (10)$$

Here  $E$  is the total energy,  $p$  the total momentum, and  $\vec{B}$  the magnetic field. The formula is obtained using the step doubling procedure outlined in Ref.

[10].

An independent limit on the error of each momentum component is not implemented because a component may reverse sign, due to the magnetic force, leading to a step size of zero at the turning point. The step size is already limited to keep the particle in the same volume and by material interactions; additional limits are unnecessary because the position is simply related to the momentum. If we take care of the momentum the position will take care of itself.

The path length parametrization of the equations of motion has a singularity at zero total momentum, but we have disregarded it. It is beyond the scope of the GEANT simulation to model the trapping of monopoles in matter. In a solenoidal field with the magnetic field parallel to the beam line it is possible for a monopole to come to a momentary complete stop, only to be accelerated by the magnetic field. But these events are irrelevant; the monopole is swept out inside the beam-pipe without reaching the detector. If a proper treatment of the singularity is needed, it can be stepped around using the time parameterization.

### *3.3 Energy loss*

After transporting the particle according to the equations of motion, the energy loss due to ionization is calculated. As shown in Section 2.3, a magnetic monopole does not obey the standard Bethe-Bloch formula. Since the monopole loss formula is related to the standard formula by a simple substitution and both depend only on  $\beta$  and not  $m$  when  $m \gg m_e$ , one can adapt

the proton loss tables and need not calculate new ones.

The energy loss for a monopole of kinetic energy  $T_{mon}$  is calculated according to the following algorithm:

- (1) Calculate the kinetic energy  $T_0$  of a proton with the same  $\beta$  as the monopole:

$$T_0 = \frac{m_p}{m_{mon}} \cdot T_{mon} .$$

- (2) Determine the index  $i$  in the energy loss table corresponding to  $T_0$  using a table  $T$  of thresholds so that <sup>2</sup>:

$$T_i < T_0 \leq T_{i+i} .$$

- (3) Compute the “proton” energy loss through linear interpolation:

$$\frac{dE}{dx}(T_0) = \frac{dE}{dx}(T_i) + \frac{T_0 - T_i}{T_{i+1} - T_i} \cdot \left( \frac{dE}{dx}(T_{i+1}) - \frac{dE}{dx}(T_i) \right) .$$

- (4) Scale the result to make it correct for monopoles:

$$\frac{dE^{mon}}{dx}(T_0) = \frac{dE}{dx}(T_0) \cdot (ng)^2 \cdot \beta^2 .$$

The first two steps and the calculation of the interpolation coefficient are already done in GEANT for charged hadrons and heavy ions in subroutine GEKBIN; we modified it to do exactly the same thing for monopoles. GTMONP performs the interpolation and the final scaling.

Figure 4 compares the energy loss curve from the GEANT table with the Bethe-Bloch formula, for both monopoles and protons. The energy loss for a monopole in GEANT agrees well with Equation 7. The curves only diverge significantly for  $\beta\gamma < 2 \cdot 10^{-2}$ , where the Bethe-Bloch formula is invalid and

<sup>2</sup>  $T$  is the array ELOW in GEANT.

GEANT uses a fit to measurements<sup>3</sup>.

The energy loss fluctuations are calculated using the standard GEANT methods [11], with the replacement of  $ze$  with  $ng\beta$  in the significance parameter  $\kappa$ , as discussed in Section 2.3.

### 3.4 Multiple Scattering

For multiple scattering, GEANT provides a Molière model, a plural scattering model, and a Gaussian model. Because the monopoles we are considering are much heavier than ordinary hadrons ( $m \geq 100 \text{ GeV}$ ), they have very small scattering angles, and we do not need the non-Gaussian tails of the full Molière model. We modified the main multiple scattering routine, **GMULTS** to use the Gaussian model, **GMGAUS**, for monopoles. For electric charges this routine calculates the RMS scattering angle:

$$\theta_0 = 2.557 \chi_{cc} ze \frac{\sqrt{d}}{E\beta^2}, \quad (11)$$

where  $\chi_{cc}$  is a characteristic of the material and  $d$  is the integration step size. The scattering angle defines a cone around the particles momentum. For isotropic materials any direction within the cone is equally likely, and so one is chosen at random. We substitute  $ng\beta$  for  $ze$  in two steps: in **GTMONP** by setting **CHCMOL** to  $\chi_{cc}ng$  instead of  $\chi_{cc}$  and in **GMULTS** by calling **GMGAUS** with

---

<sup>3</sup> After version 3.15 GEANT does not use direct linear interpolation of the energy loss tables for standard particles but uses stopping range tables instead. This is done in order to avoid overestimating energy losses near the  $\beta = 0$  singularity of the Bethe-Bloch equation. Monopoles do not have this singularity so the older method is still applicable.

$\beta$  instead of  $\beta^2$ . These substitutions are made only for monopoles (ITRTYP=9).

## 4 Code Validation

One cannot—at least yet—compare the GEANT simulation with real data, meaning that cross checks are the only available tool for validating the code. We compare the GEANT code with a simpler monopole simulation and compare the Runge-Kutta integration with the analytic solution. None of these checks validate the assumptions and models discussed in the previous sections; they merely check for mistakes in the implementation.

### 4.1 Comparison with a Simple Simulation

We created a simple monopole simulation using ROOT [12], called MonSim, which is completely independent from GEANT. MonSim uses a simplified detector geometry with most regions modeled as uniform cylinders. It treats the energy loss using the monopole Bethe-Bloch formula (Equation 7) and multiple scattering using the Gaussian model (Section 2.4). It also assumes the magnetic field is uniform and in the  $+z$  direction. In this case, the equation of motion has an analytic solution:

$$\vec{r}(t) = \frac{E_{t_0}}{gB} \left( \sqrt{1 + \left(\frac{gB}{E_{t_0}}(t + \Delta t)\right)^2} - \sqrt{1 + \left(\frac{gB}{E_{t_0}}\Delta t\right)^2} \right) \vec{e}_z + \frac{p_{t_0}}{gB} \cdot \left( \operatorname{arsinh}\left(\frac{gB}{E_{t_0}}(t + \Delta t)\right) - \operatorname{arsinh}\left(\frac{gB}{E_{t_0}}\Delta t\right) \right) \vec{e}_t, \quad (12)$$

where  $E_{t_0}$  is the initial transverse energy and  $p_{z_0}$  is the initial value of the monopole's  $z$  component of momentum. The time it takes the magnetic field

to change  $p_z$  from zero to  $p_{z_0}$  is  $\Delta t = p_{z_0}/gB$ . The special solution with  $p_{z_0} = 0$  is easily calculated; the general solution is obtained by advancing the special solution by the time  $\Delta t$ .

As a test case we use the CDF detector, which has been described in detail elsewhere [13a–b]. CDF’s new Time-of-Flight (TOF) detector, built to enhance particle identification, is of particular interest, as it has been used for a magnetic monopole trigger [14]. The TOF consists of 216 bars of fast scintillator, 3.0 m in length, forming a cylinder between the COT chamber and the solenoid. A slightly trapezoidal cross sections reduces the size of cracks between bars. Photomultiplier tubes (PMTs) are mounted on both ends of each bar along with signal boosting preamplifiers. Because PMT gains are substantially reduced in magnetic fields, the PMT’s are of a special high gain design. The highly ionizing nature of magnetic monopoles leads to large light production in scintillators, providing an excellent trigger opportunity.

For the comparison, we used a simplified model of the CDF detector, consisting of the beam-pipe, central tracker, TOF detector, and solenoid. This geometry was implemented in MonSim, and all additional components were omitted from the GEANT geometry. We take the proton direction along the beam-pipe as  $+z$ , upward as  $+y$ , and the usual azimuthal angle as  $\phi$ .

Monopole pair events with identical initial conditions were simulated in both programs. The acceptance of the TOF system across a range of monopole masses is shown in Figure 6 as measured by both programs; they are in good agreement as to whether or not a monopole hits the TOF scintillators. The difference between GEANT and MonSim calculations of the  $E$ ,  $z$ , and  $\phi$  of the monopole at the radius of the TOF scintillator are shown in Figure 7, Figure

8, and Figure 9 for a monopole with 500 GeV mass. The trajectory and energy dependence of single typical event is shown in Figure 10 and Figure 11. The agreement between the two programs is excellent.

There are some tails in the distributions, however. One tail event is shown in Figure 12 and Figure 13. At the turning point, the monopole has very little energy, and the discrepancy between the Bethe-Bloch formula and the GEANT tables becomes noticeable (Figure 4). The later rapid acceleration of the monopole has the effect of magnifying this small difference. Even for tail events, the discrepancy is less than 1% of the total energy of the particle.

#### *4.2 Comparison between analytic and Runge-Kutta solutions*

As an additional cross check, we compare both GEANT implementations: the analytic solution **GPARMP** and the Runge-Kutta integration **GRKTMP**. As in the previous section, we compare the Energy (Figure 14),  $z$  (Figure 15), and  $\phi$  (Figure 16) difference at the TOF radius. The results are in excellent agreement, with slightly asymmetric tails due to the assumption, in **GPARMP**, that the magnetic field is in the  $z$  direction only.

## **5 Conclusions**

The extension of classical electromagnetism to include magnetic charge leads to a symmetry between electric and magnetic quantities. This symmetry can be exploited to deduce magnetic interactions from electric ones in a straightforward way. Using this model, GEANT has been extended in a consistent fashion to handle magnetic monopoles. We have tested our GEANT imple-

mentation against a much simpler monopole dedicated simulation. The two independent programs are in excellent agreement.

The magnetic monopole extension to GEANT is available for download from <http://fcdfhome.fnal.gov/usr/mulhearn/geant-monopoles/>. We have made this extension to assist in a direct search for magnetic monopoles at CDF, from which we will publish results shortly.

## References

- [1] P.A.M. Dirac, *Quantized Singularities In The Electromagnetic Field*, Proc. R. Soc. (London), A133 (1931).
- [2a] I. De Mitri, *Search For Magnetic Monopoles in the Cosmic Radiation with the Macro Detector at Gran Sasso*, Budapest 2001, High energy physics, hep2001/213.
- [2b] S. Cecchini et al., *Search for Magnetic Monopoles at the Chacaltaya Cosmic Ray Laboratory*, Nuovo Cim.24C:639-644 (2001).
- [2c] S.D. Wick, T.W. Kephart, T.J. Weiler, P.L. Biermann, *Signatures for a Cosmic Flux of Magnetic Monopoles*, astro-ph/0001233 (2000).
- [3a] I.F. Ginzburg, A. Schiller, *Search For a Heavy Magnetic Monopole at the Tevatron and LHC*, Phys.Rev.D57:6599-6603 (1998), HEP-PH 9802310.
- [3b] B. Abbot et al, *A Search for Heavy Point like Dirac Monopoles*, Fermilab-Pub-98/095-E (1998).
- [3c] M. Acciarri et al., *Search for Anomalous  $Z \rightarrow \gamma\gamma\gamma$  Events at Lep*, Phys. Lett. B345, 609-616 (1995).

- [3d] L. Gamberg, G.R. Kalbfleisch, K.A. Milton, *Direct and Indirect Searches for Low-Mass Magnetic Monopoles*, hep-ph/9906526, (1999).
- [4] G.R. Kalbfleisch, W. Luo, K.A. Milton, E.H. Smith, M.G. Strauss, *Limits on Production of Magnetic Monopoles Utilizing Samples from the D0 and CDF Detectors at the Tevatron*, hep-ex/0306045.
- [5] G. Giacomelli, L. Patrizii, *Magnetic Monopole Searches*, Trieste 2002, Astroparticle physics and cosmology 121-144, hep-ex/0302011.
- [6a] J. Schwinger, K.A. Milton, W. Tsai, L.L. DeRaad, D.C. Clark, *Nonrelativistic Dyon-Dyon Scattering*, Ann. Phys. (N.Y.) 101, 451 (1976)
- [6b] L. Gamberg, K.A. Milton, *Dual quantum electrodynamics: Dyon-dyon and charge-monopole scattering in a high-energy approximation*, Phys. Rev. D 61, (2000).
- [6c] L. Gamberg, K.A. Milton, *Eikonal scattering of monopoles and dyons in dual QED*, OKHEP-00-05, (2000).
- [7] Particle Data Group, Eur. Phys. J. C3, 144 (1998).
- [8] J.D. Jackson, *Classical Electrodynamics*, Second Edition. New York: de Gruyter, (1982).
- [9a] J. Schwinger, L.L. DeRaad Jr., K.A. Milton, W. Tsai, *Classical Electrodynamics*, Reading, MA: Perseus Books, (1998).
- [9b] M.E. Peskin, D.V. Schroeder, *An Introduction to Quantum Field Theory*, Reading, MA: Perseus Books, (1995).
- [9c] W. Greiner, J. Rafelski, *Spezielle Relativitätstheorie*, 3. überarb. Auflage. Frankfurt: Harri Deutsch, (1992).
- [10] W.H. Press, B.P. Flannery, S.A. Teukolsky, W.T. Vetterling, *Numerical Recipes in Pascal*, Cambridge University Press, (1989).

- [11] *GEANT Detector Description and Simulation Tool*, CERN Program Library Writeup W5013, (1994).
- [12] Rene Brun and Fons Rademakers,  
ROOT - An Object Oriented Data Analysis Framework,  
Proceedings AIHENP'96 Workshop, Lausanne, Sep. 1996, Nucl. Inst. & Meth.  
in Phys. Res. A 389 (1997) 81-86. See also <http://root.cern.ch/>.
- [13a] CDF Run II Technical Design Report.  
On the WEB under: <http://www-cdf.fnal.gov/upgrades/tdr/tdr.html>
- [13b] CDF Collaboration, *A Time-Of-Flight System for CDF*, FERMILAB-PROPOSAL-0830-3 (1995).
- [14] M.J. Mulhearn, Ph.D. dissertation, Massachusetts Institute of Technology, 2004.
- [15] Torbjorn Sjostrand, *Pythia 5.7 and Jetset 7.4 Physics and Manual*, (1998).

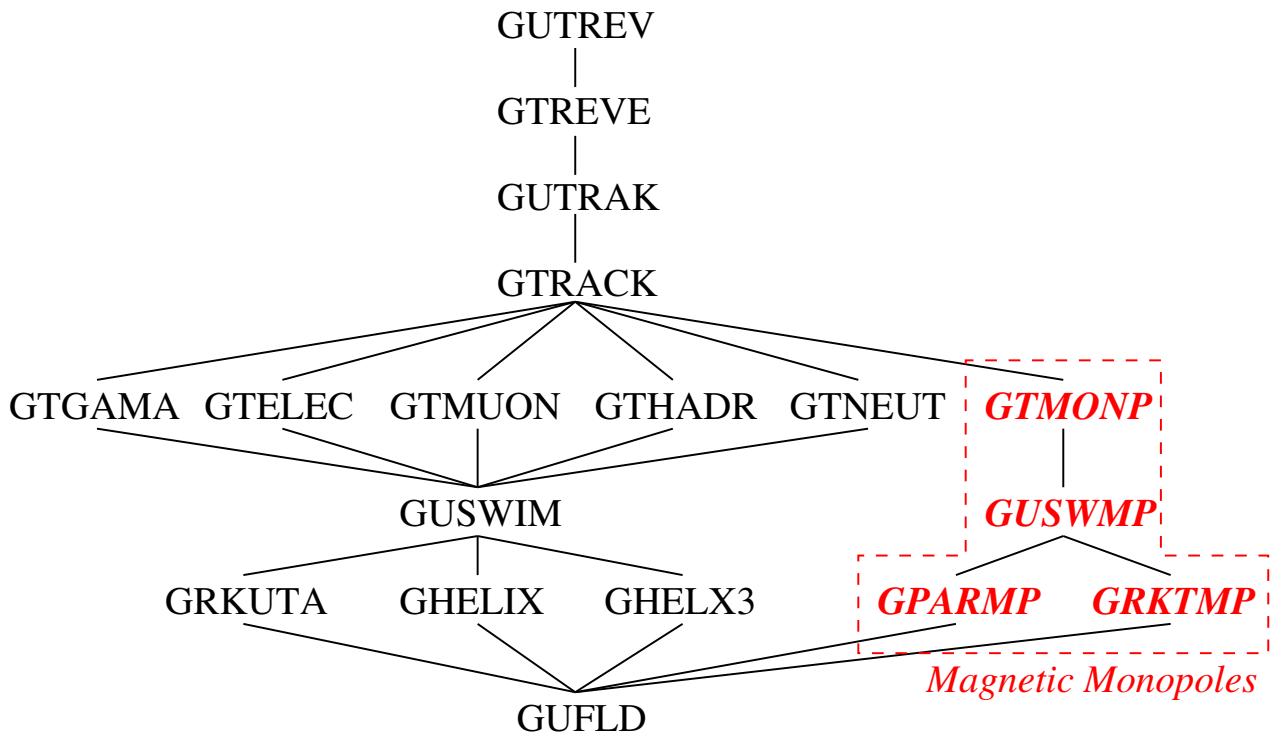


Fig. 1.

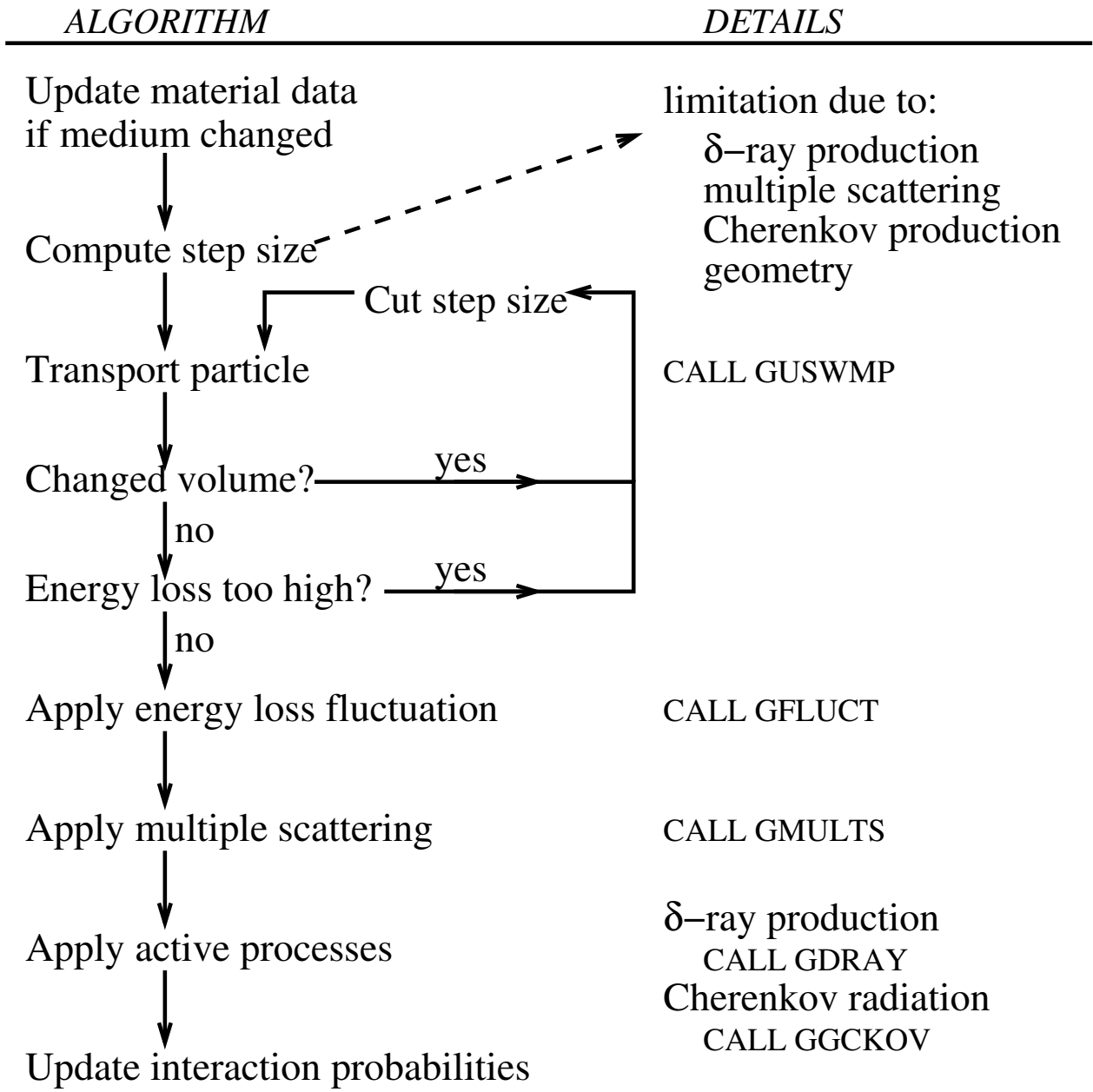


Fig. 2.

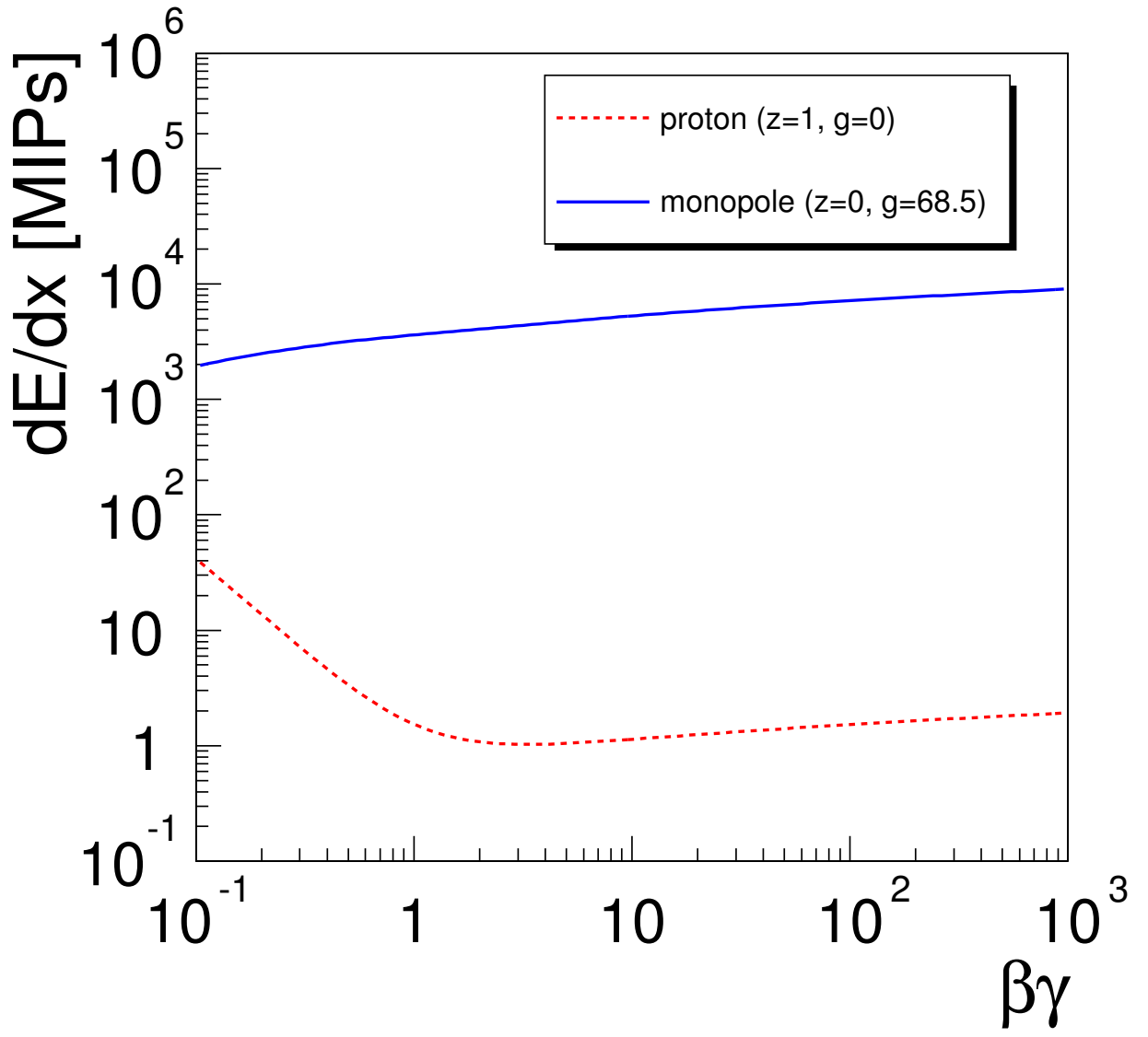


Fig. 3.

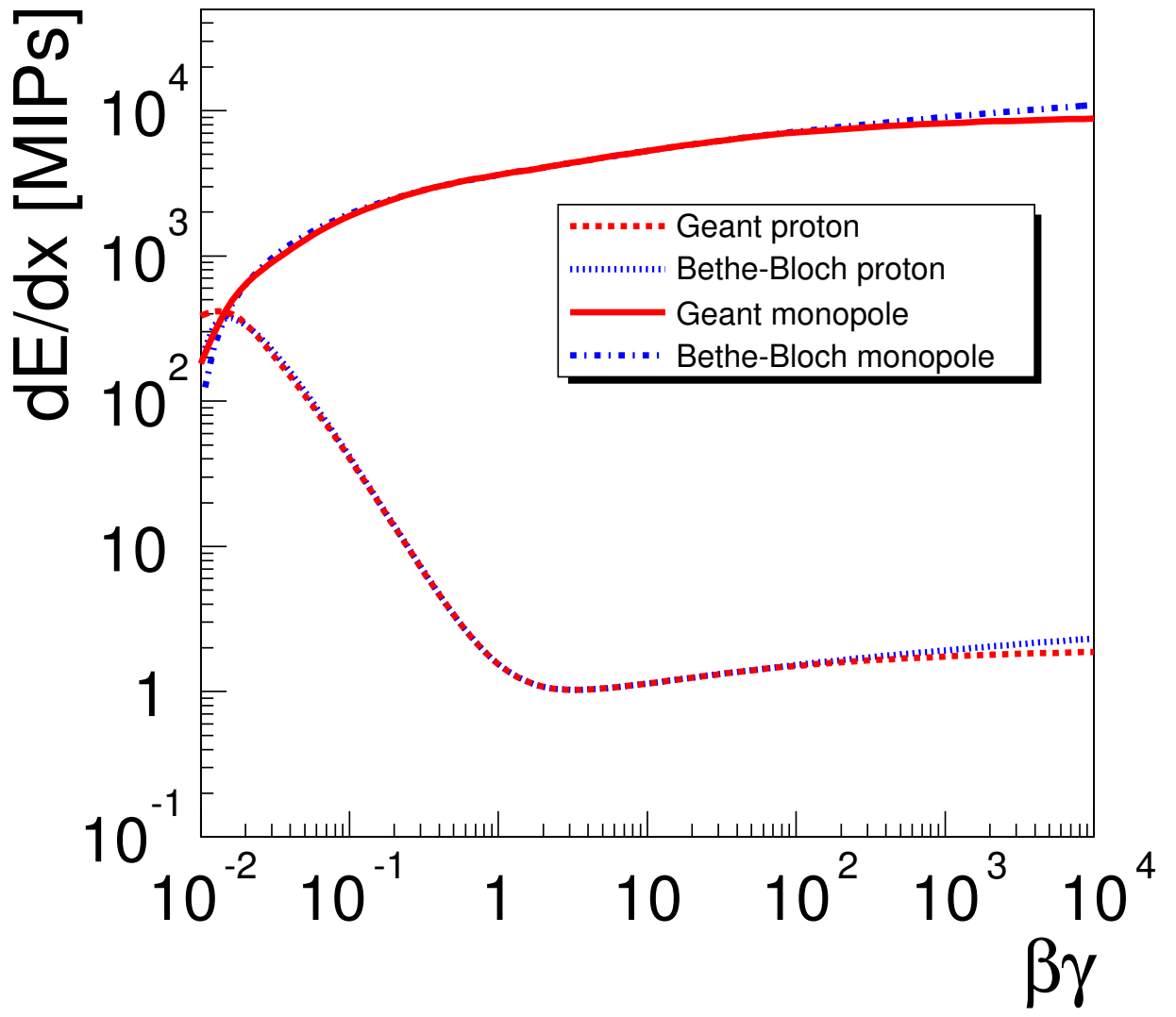


Fig. 4.

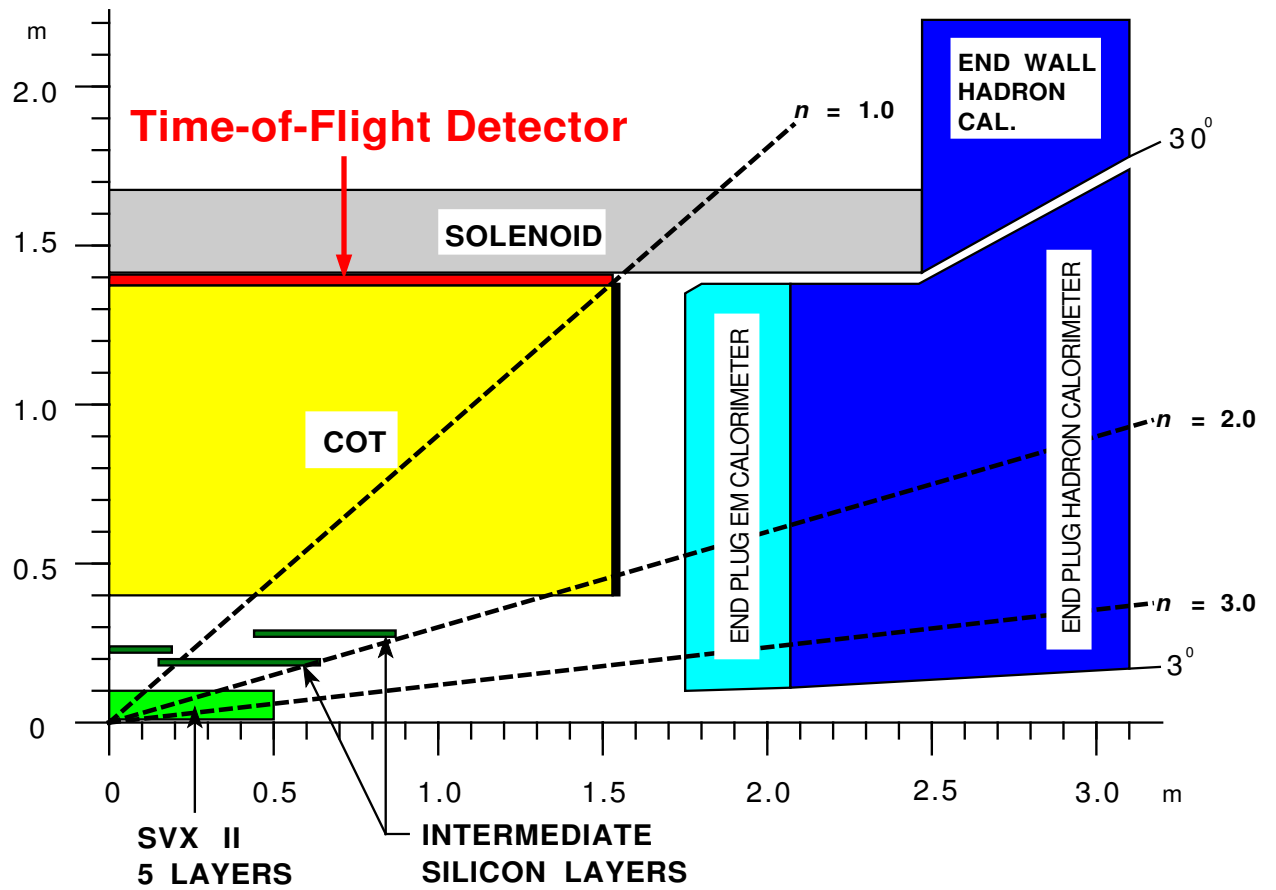


Fig. 5.

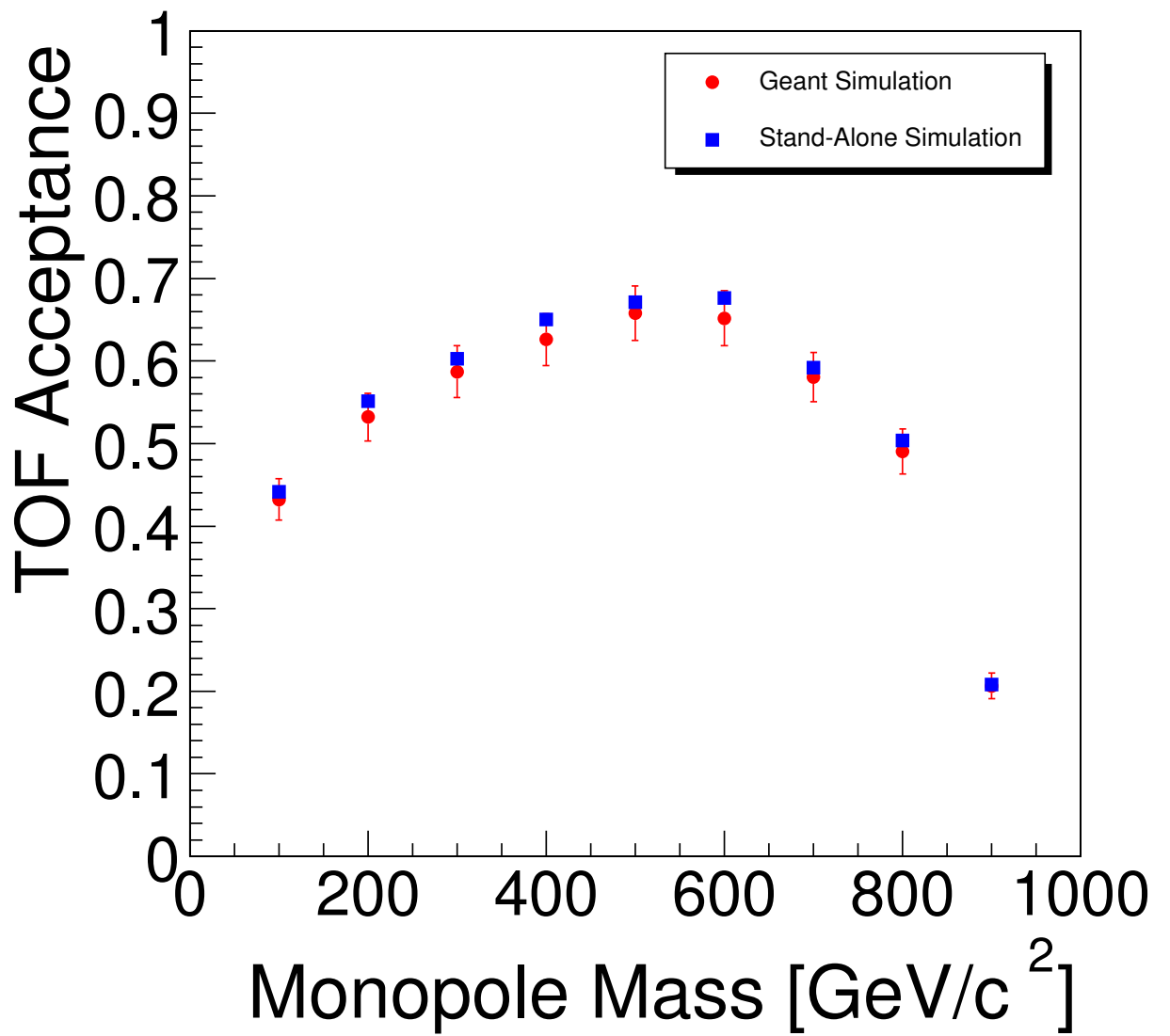


Fig. 6.

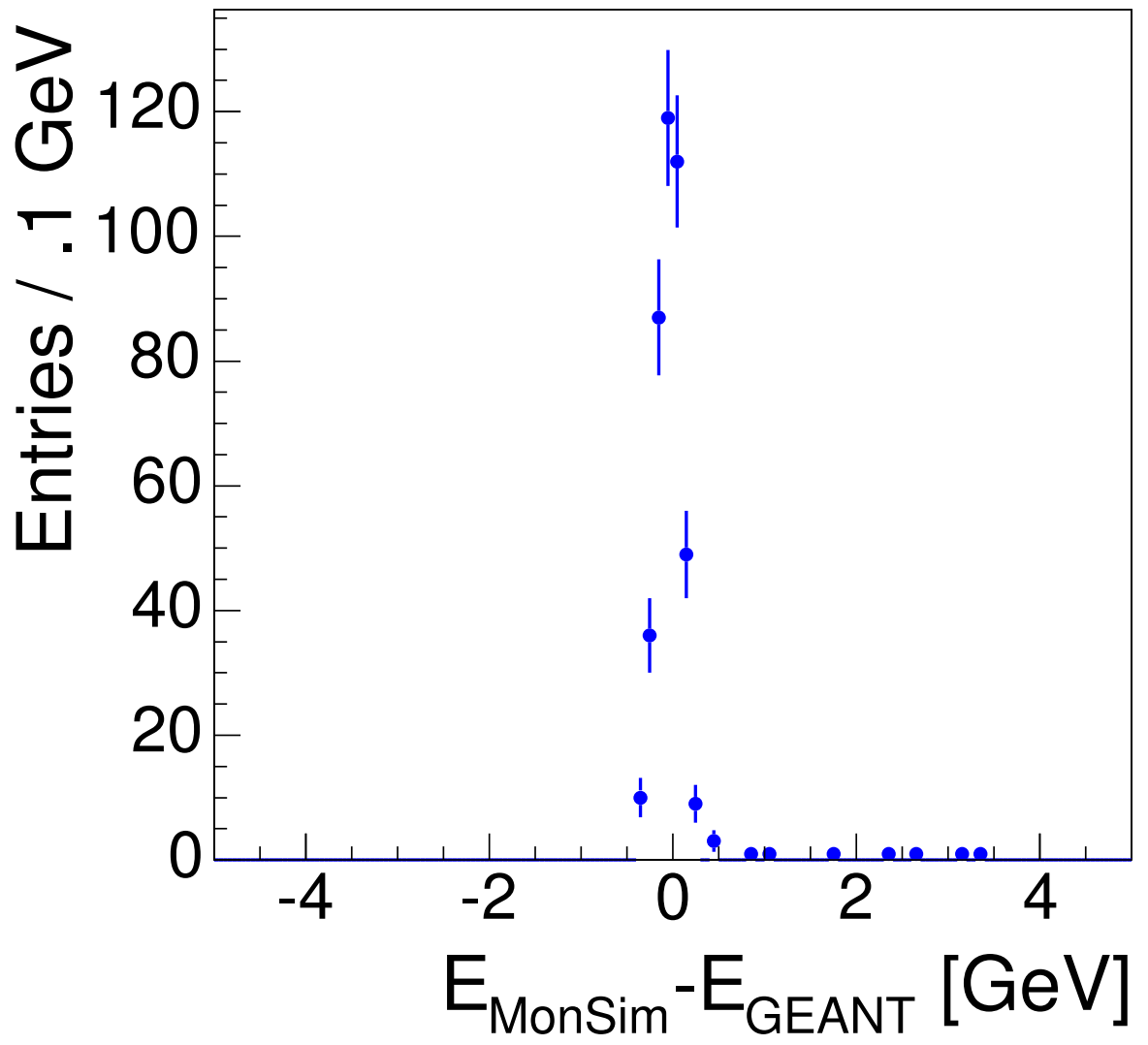


Fig. 7.

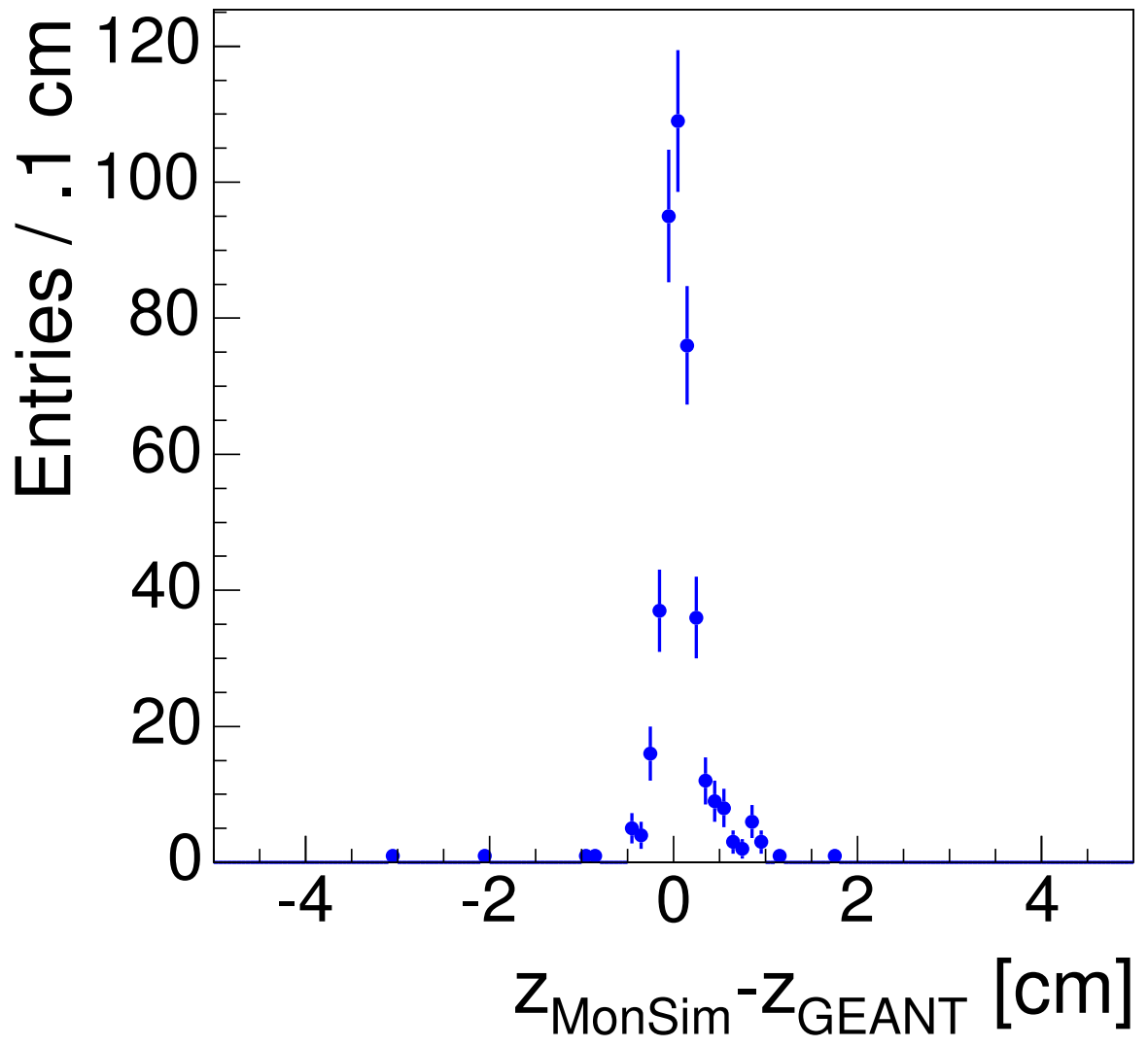


Fig. 8.

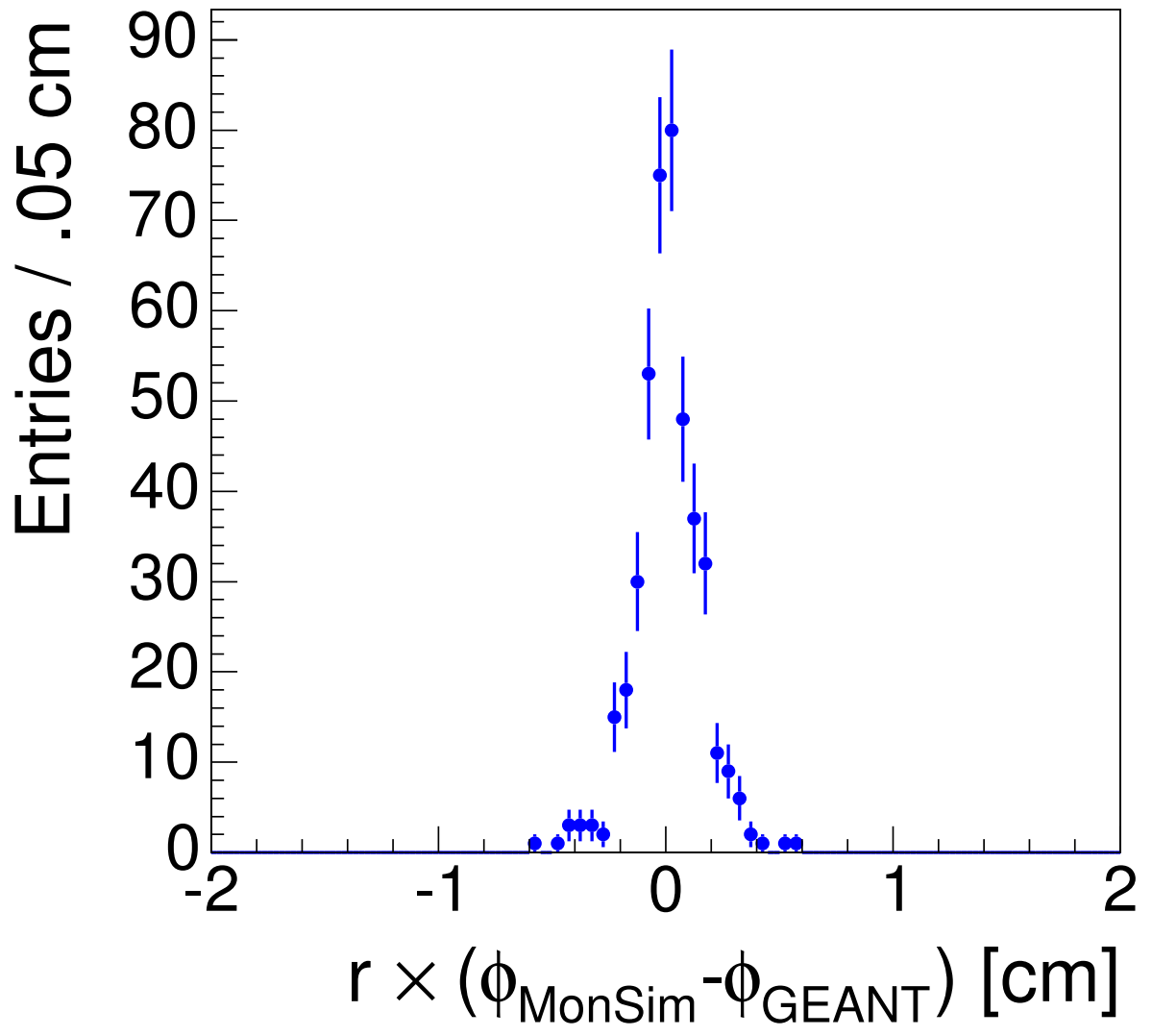


Fig. 9.

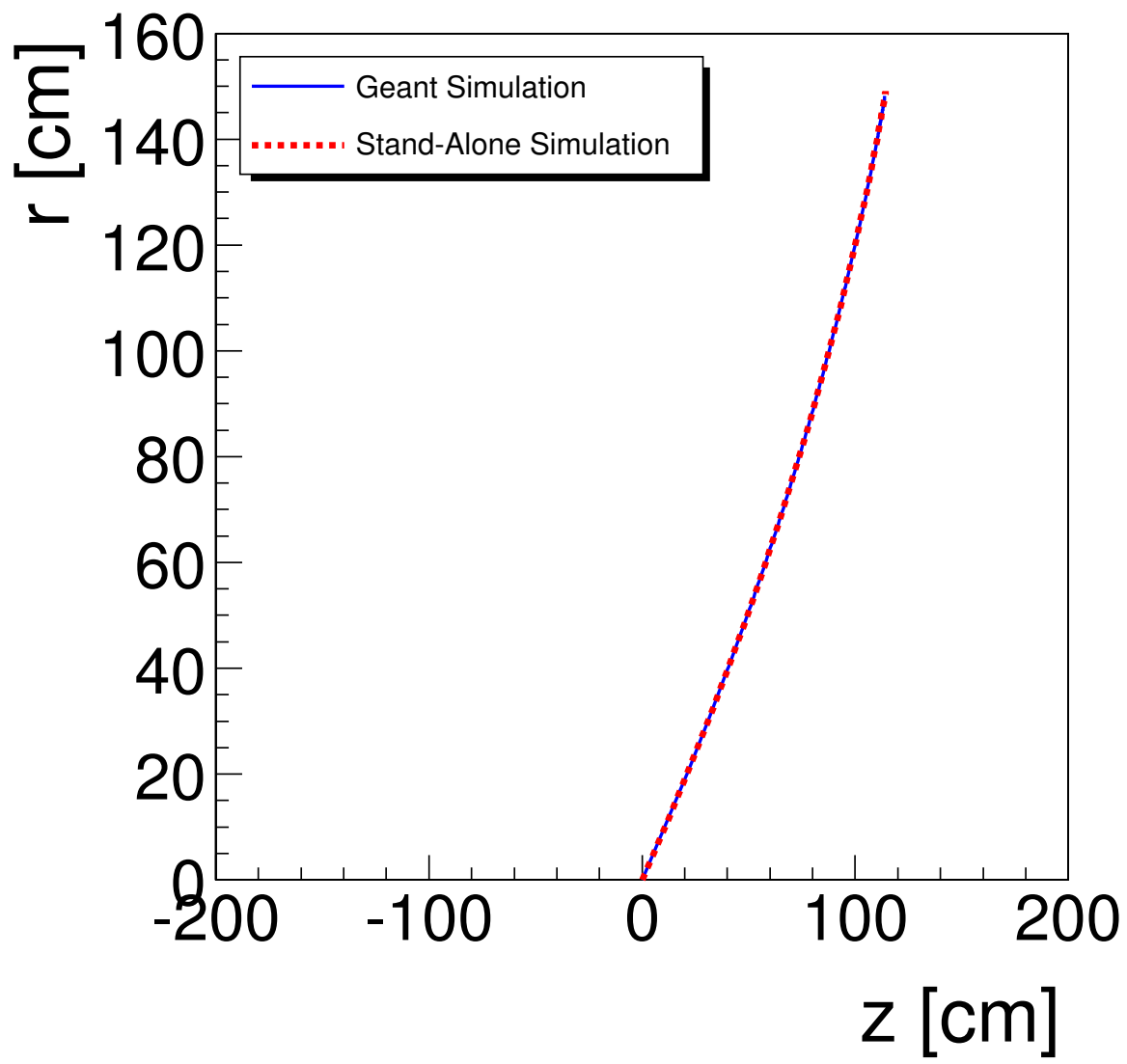


Fig. 10.

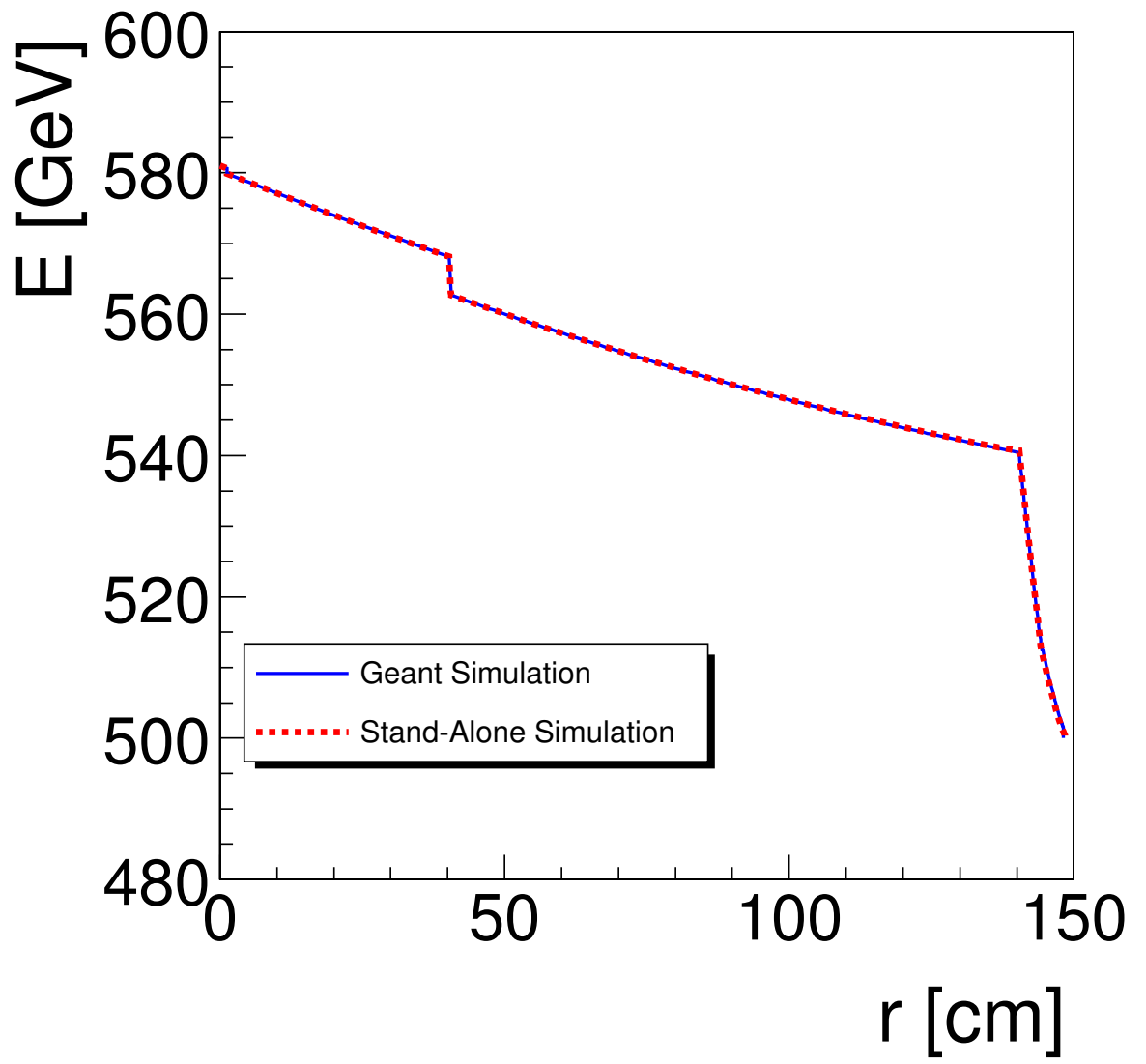


Fig. 11.

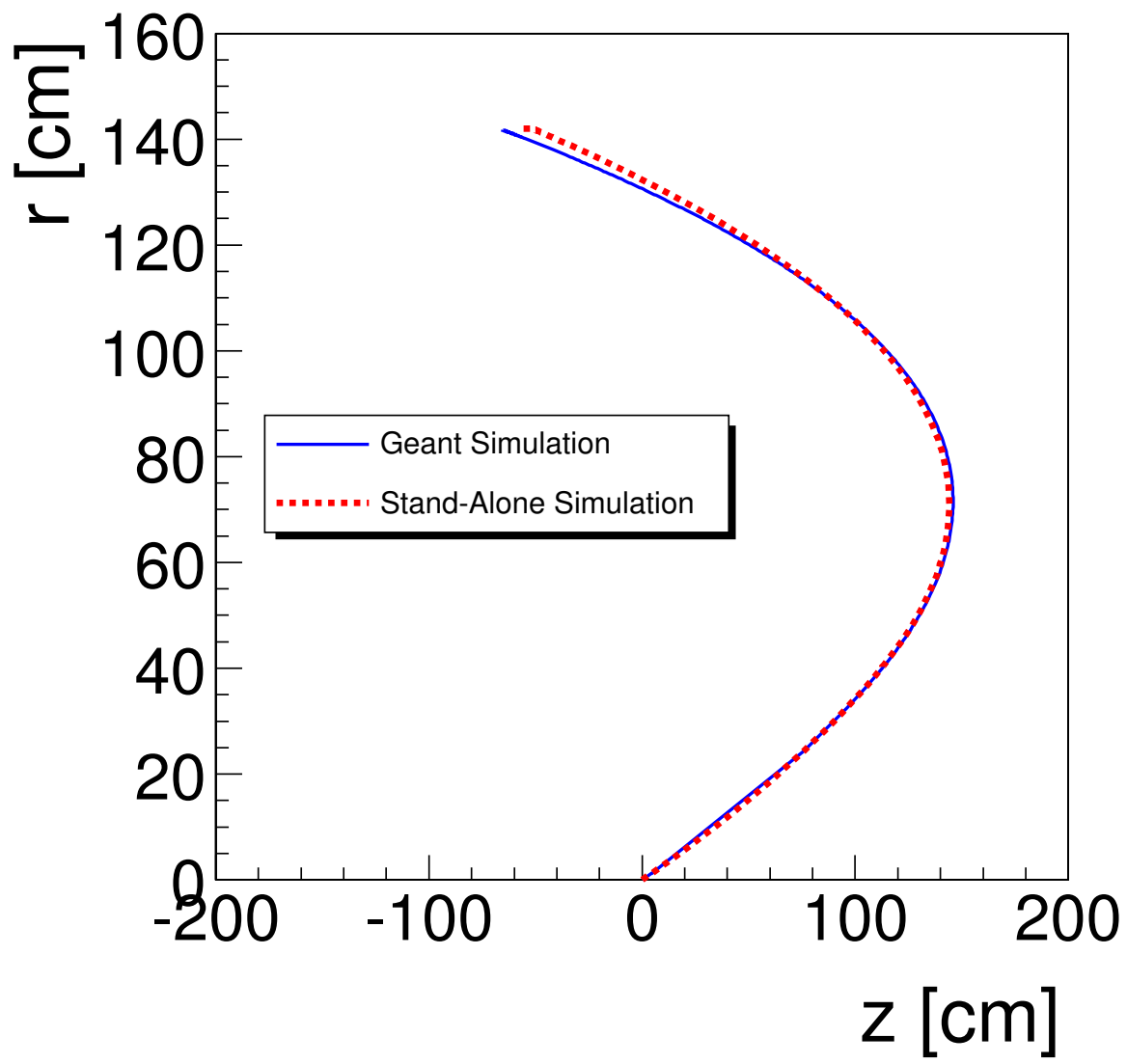


Fig. 12.

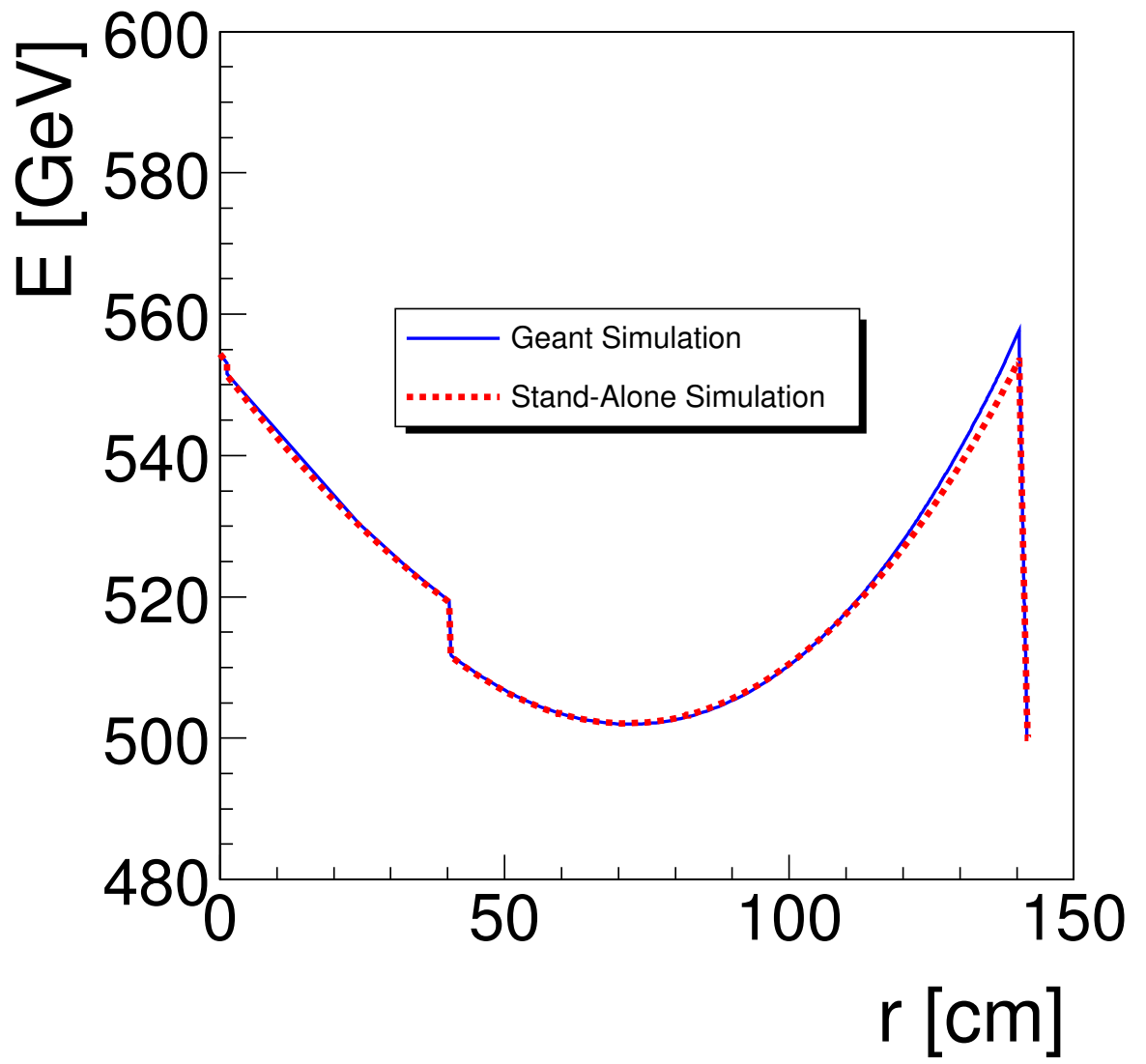


Fig. 13.

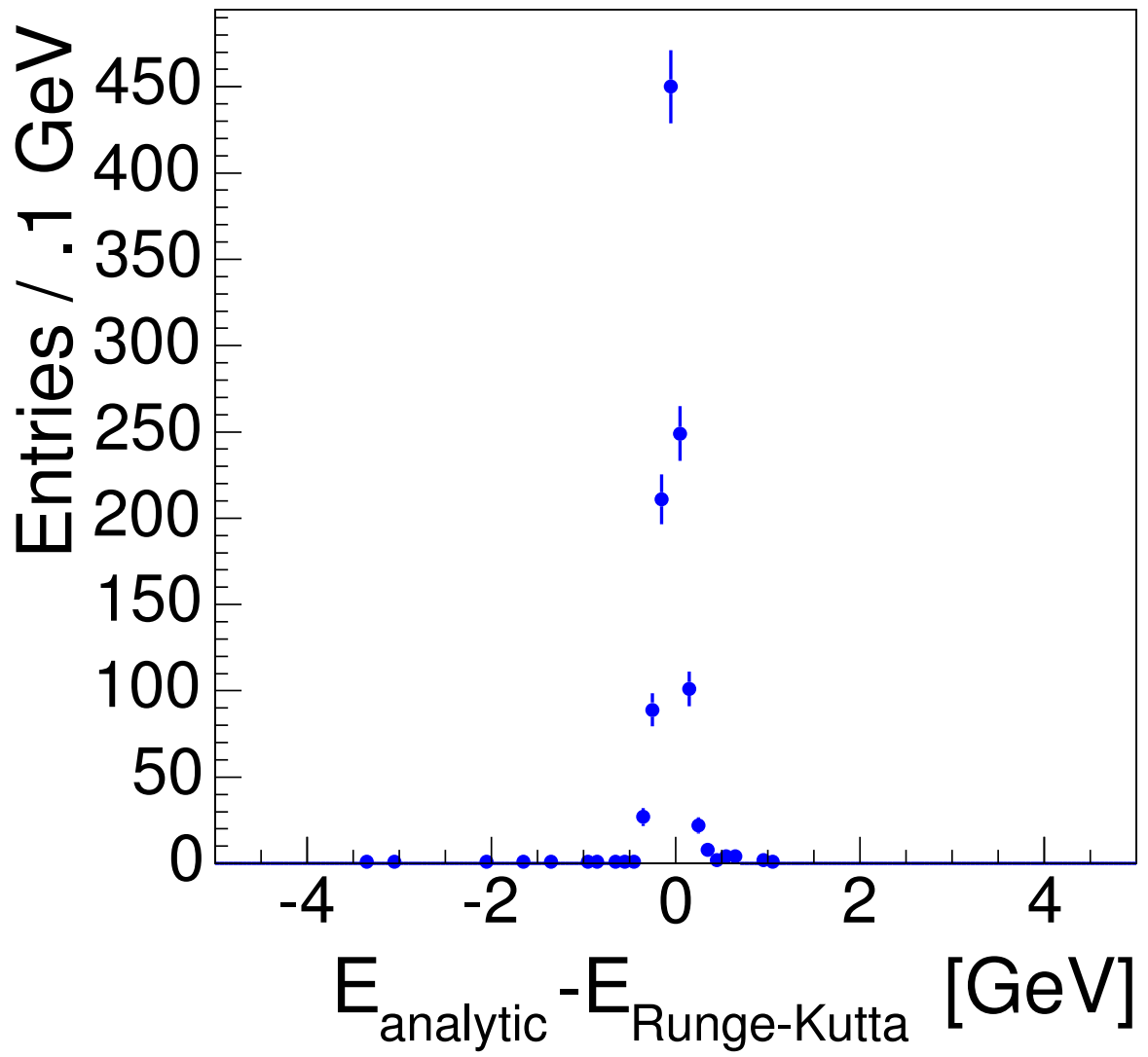


Fig. 14.

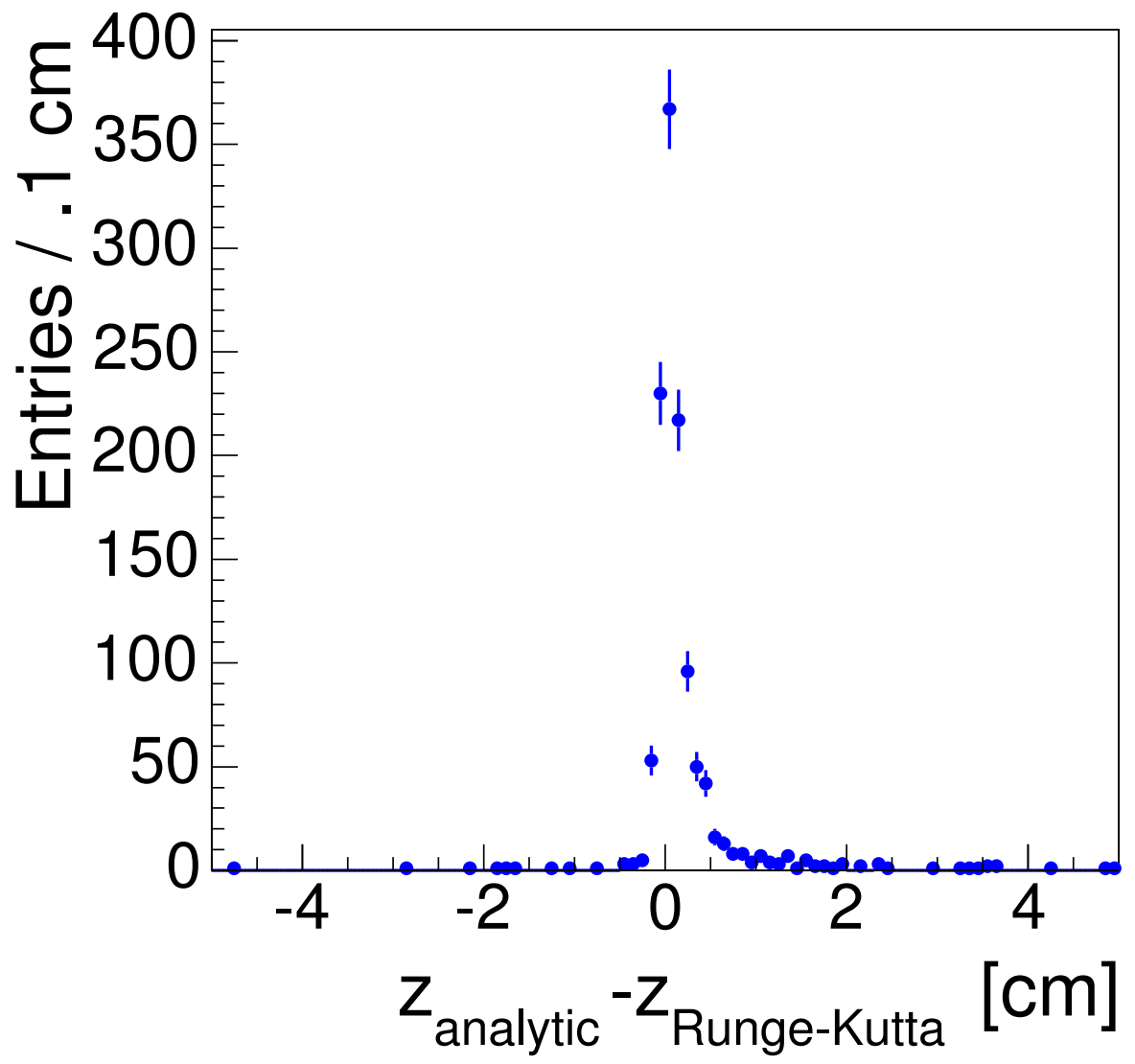


Fig. 15.

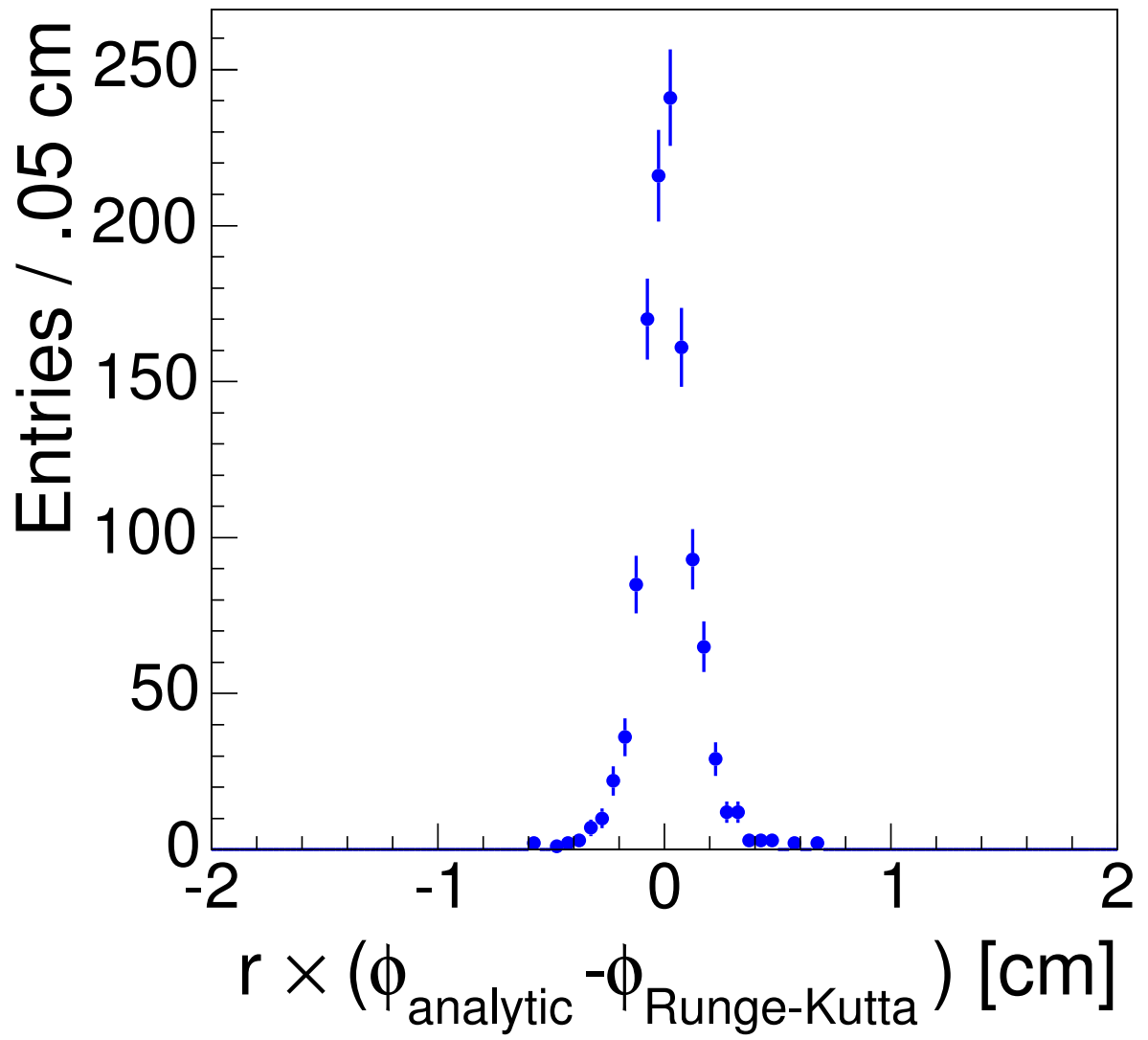


Fig. 16.

## 6 Figure Captions

- (1) The structure of the GEANT tracking package.
- (2) The algorithm for the monopole tracking routine GTMONP.
- (3) The energy loss of electric and magnetic charges in air.
- (4) A comparison of the Bethe-Bloch formula with GEANT tables for the energy loss of monopoles and protons in air.
- (5) A sectional view of CDF, including the integrated tracking system.
- (6) A comparison of the TOF acceptance for GEANT and MonSim.
- (7) The total energy difference at the TOF radius for GEANT and MonSim.
- (8) The  $z$  difference at the TOF radius for GEANT and MonSim.
- (9) The  $\phi$  difference at the TOF radius for GEANT and MonSim.
- (10) The monopole trajectories in  $r$ - $z$  for a typical event.
- (11) The monopole energy versus radial distance for Figure 10. The large kinks are due to rapid energy loss at the COT inner cylinder and TOF scintillator bars.
- (12) The monopole trajectories in  $r$ - $z$  for an event with a large  $z$ -displacement of 12.0 cm at TOF radius.
- (13) The monopole energies versus radial distance for Figure 12.
- (14) The total energy difference at TOF radius for the analytic and Runge-Kutta GEANT implementations.
- (15) The  $z$  difference at the TOF radius for the analytic and Runge-Kutta GEANT implementations.
- (16) The  $\phi$  difference at the TOF radius for the analytic and Runge-Kutta GEANT implementations.